Cavitation on a scaled-down model of a Francis turbine guide vane: high-speed imaging and PIV measurements

K S Pervunin[1,2], M V Timoshevskiy[1,2], S A Churkin[1,2], A Yu Kravtsova[1,2], D M Markovich[1,2,3] and K Hanjalić[2,4]

[1] Kutateladze Institute of Thermophysics, SB RAS, 1, Lavrentyev Ave., Novosibirsk, 630090, Russia
[2] Department of Physics, Novosibirsk State University, 2, Pirogov Str., Novosibirsk, 630090, Russia
[3] Institute of Power Engineering, Tomsk Polytechnic University, 30, Lenin Ave., Tomsk, 634050, Russia
[4] Department of Chemical Engineering, Delft University of Technology, 136, Julianalaan, Delft, 2628 BL, the Netherlands

pervunin@itp.nsc.ru

Abstract. Cavitation on two symmetric foils, a NACA0015 hydrofoil and a scaled-down model of a Francis turbine guide vane (GV), was investigated by high-speed visualization and PIV. At small attack angles the differences between the profiles of the mean and fluctuating velocities for both hydrofoils were shown to be insignificant. However, at the higher angle of incidence, flow separation from the GV surface was discovered for quasi-steady regimes including cavitation-free and cavitation inception cases. The flow separation leads to the appearance of a second maximum in velocity fluctuations distributions downstream far from the GV surface. When the transition to unsteady regimes occurred, the velocity distributions became quite similar for both foils. Additionally, for the GV an unsteady regime characterized by asymmetric spanwise variations of the sheet cavity length along with alternating periodic detachments of clouds between the sidewalls of the test channel was for the first time visualized. This asymmetric behaviour is very likely to be governed by the cross instability that was recently described by Decaix and Goncalvès [8]. Moreover, it was concluded that the existence of the cross instability is independent on the test body shape and its aspect ratio.

1. Introduction

Despite a relatively large set of common attributes, cavitating flows around bodies of quite similar shape and the same size can have different features. Investigations of those are particularly necessary in cases when the test body is a foil shaped to reproduce a 2D vane or 3D blade (even for scaled-down models) used in real full-scale hydrotechnical systems. In various experimental and numerical works, spatial structure and dynamics of cavities on generic symmetric bodies are described (e.g., [1-3]) and distributions of the mean and turbulence characteristics around them are presented (e.g., [4-6]). However, results for guide vanes and/or rotor blades are not available in literature yet.

The current work aims at a detailed analysis of high-speed imaging data on spatial structure and dynamics of gas-vapor cavities and results of PIV measurements around a cavitating scaled-down model of symmetric guide vanes used in high-pressure hydroturbines and a comparison with those for a well-studied NACA0015 series hydrofoil with the same chord length.

2. Experimental conditions and measurement techniques

The experiments were carried out at the Cavitation tunnel in Kutateladze Institute of Thermophysics SB RAS with the test channel cross-section ($H \times W$) of 250×80 mm. Its description can be found in [7] as well as details on experimental conditions and measurement techniques applied. In tests, the attack angle α = 0, 3 and 9° and the cavitation number σ were changed to register various cavitation regimes on the test bodies. The Reynolds number was between 0.9×10^6 and 1.7×10^6. The test bodies (figure 1) – NACA0015 hydrofoil and scaled-down model of a guide vane (GV) – are made of brass with the same surface roughness of 1.5 mm. Their chord C and span lengths are 100 and 80 mm, respectively. The maximum width of GV is 0.2148C at the distance of 0.43C from the leading edge. The rounding radius of the leading part is 2.48 mm for the NACA0015 foil and 1.97 mm for the guide vane model.

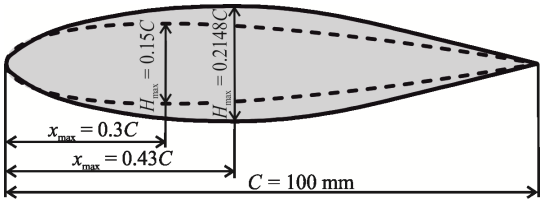

Figure 1. A schematic diagram of the test bodies: a NACA0015 series hydrofoil (dashed line) and scaled-down model of a guide vane (solid line).

3. Results

3.1. Visualization

At α = 9°, cavitation on the GV section initiates at roughly σ = 2.87 as a streak array (their length is quite small (≈ 0.02C), whereas on the NACA0015 hydrofoil it occurs at σ = 3.03 in form of isolated and elongated bubbles (figure 2-b.1), their length is about 0.08C. Unlike those, streaks on the GV are located very close to each other forming a cavity over the whole foil span. When σ = 2.49, the cavity length on the GV section increases up to 0.16C (figure 2-a.1). On the NACA foil, a decrease of σ down to 2.48 (figure 2-b.2) leads to a change of cavitation pattern from elongated bubbles to streaks, which emerge into small clouds downstream, so that an entire cavity (L_C/C = 0.24) is formed.

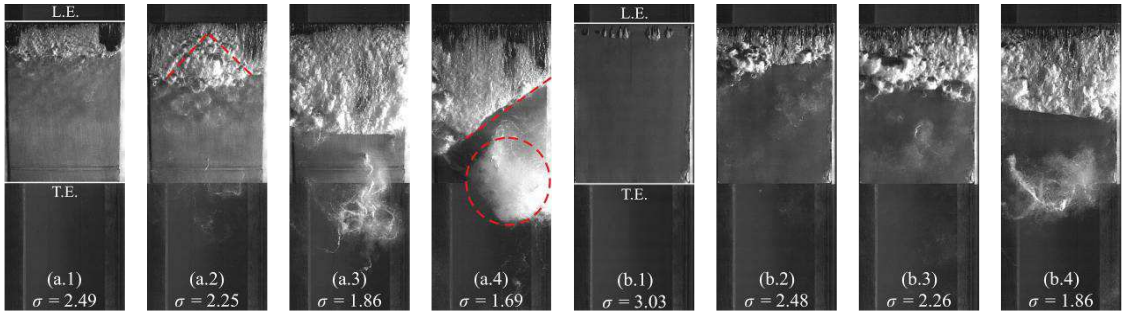

Figure 2. Instantaneous images of partial cavities (top view) on the suction side of (a) the GV when (a.1) σ = 2.49, L_C/C = 0.16 (attached cavity), (a.2) σ = 2.25, L_C/C = 0.37 (transitional cavitation), (a.3) σ = 1.86, L_C/C = 0.65, St = 0.29 (cloud cavitation), (a.4) σ = 1.69, L_C/C = 0.8, St = 0.27 (asymmetric cloud shedding) and (b) the NACA0015 hydrofoil when (b.1) σ = 3.03, L_C/C = 0.075 (isolated bubbles), (b.2) σ = 2.48, L_C/C = 0.24 (attached cavity), (b.3) σ = 2.26, L_C/C = 0.33 (transitional cavitation), (b.4) σ = 1.86, L_C/C = 0.54, St = 0.47 (typical cloud cavitation). α = 9°. The flow is from above.

Transition to unsteady regimes on both foils occurs when σ decreases down to 2.05. All unsteady regimes registered on the hydrofoils at $\alpha = 9°$ were of cloud-type. This means that intrinsic instabilities totally determine the attached cavity behaviour on both hydrofoils at large incidence angles (for details see [7]). Typical Strouhal number is 0.47 for the NACA foil when $\sigma = 1.86$ (figure 2-b.4), whereas it is 0.29 for the GV section at the same cavitation number (figure 2-a.3). Moreover, when the cavitation number was decreased down to 1.69, a variation of the attached cavity length in the spanwise direction in any phase of the cavity growth-reduction cycle was discovered for the GV section (see figure 2-a.4). The evolution of this extraordinary regime is presented in figure 3 within a full period of cavity length oscillations.

This transient, essentially 3D regime is characterized by alternating periodic asymmetric shedding of clouds from one side of the GV in spanwise direction and then from the other. Moreover, it is transient and seems to suffer a bifurcation behavior. As a result, a transition to cloud cavitation finally occurs. According to numerical calculations by Decaix and Goncalvès [8], this asymmetric behavior is very likely to be governed by the cross instability. Additionally, comparing the test object and its AR in our experiment with those in the work [8], the existence of the cross instability is highly probably independent on the test body shape and its aspect ratio.

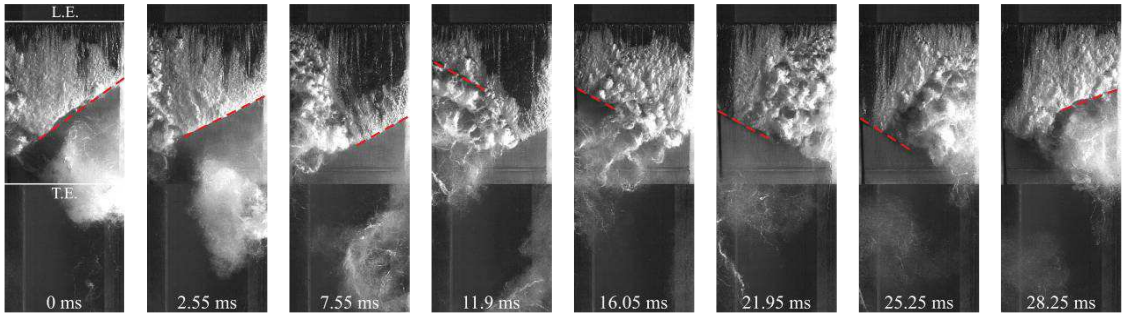

Figure 3. Time-series of growth-reduction cycle of unsteady cavity (top view) on the suction side of the GV at $\alpha = 9°$ for $\sigma = 1.69$ ($L_C/C = 0.8$, St = 0.27, $T = 28.35$ ms). The flow is from above.

3.2. Velocity distributions

In case of the single-phase flow around the NACA foil at $\alpha = 9°$, the transverse dimension of the boundary layer is roughly $0.08C$ for $x/C = 1$ that is very close to the case at $\alpha = 3°$. However, its dimension over the GV section at $\alpha = 9°$ is about 2 times wider than that at $\alpha = 3°$ in the same cross-section (figure 4-a). Such a significant modification of the boundary layer over the GV model is caused by flow separation from its surface at $x/C \approx 0.71$, which also leads to the appearance of the second maximum in the velocity fluctuations above the trailing edge of the vane (at $y/C = 0.1$). The amplitude of turbulent velocity fluctuations rises up to $\tilde{u}/U_0 = 0.3$ in the wake ($x/C > 1$) of the GV model (figure 4-a).

When the cavitation develops (figure 4-b), the velocity distributions alter substantially and the position of the separation point on the GV changes continually. Therefore, the separation was not registered in the average velocity fields. Moreover, the cavity length on the GV model becomes equivalent to (figure 4-b) or even larger by approximately 25% than that on the NACA foil. At $x/C = 0.7$ the maxima of the velocity fluctuations are quite close for both foils ($\tilde{u}/U_0 = 0.23$) in the near-wall region, but further away from the foil surface ($y/C > 0.02$) $\tilde{u}/U_0$ is significantly higher over the NACA foil because here the boundary layer is about three times thicker ($0.12C$) than on the GV model ($0.04C$). At the trailing edge (figure 4-c), velocity fluctuations increase up to $\tilde{u}/U_0 = 0.3$ on the GV model, which is approximately 50% higher than in the case of the NACA foil. Transition to the cloud cavitation leads to the appearance of intensive quasi-periodic pulsations of the gas-vapor cavity length and probably because of this the velocity distributions become quite similar (not presented). The amplitude of velocity fluctuations grows up to $\tilde{u}/U_0 = 0.3$ over both foils ($0.4 < x/C < 0.7$) but past the foils ($x/C > 1$) the profiles almost coincide.

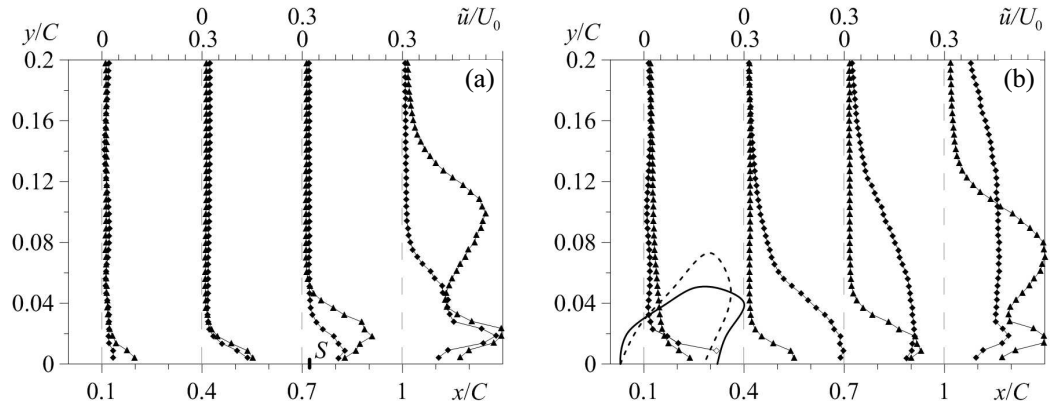

Figure 4. Downstream evolution of the streamwise turbulence intensity (rms-values) for (a) cavitation-free flow at σ = 3.41 (GV) and 3.35 (NACA0015) and (b) transitional cavitation at σ = 2.25 (GV) and 2.26 (NACA0015). α = 9°. ▲ – GV and ◆ – NACA0015. Solid and dashed lines represent time-averaged interfaces of the attached cavities on the GV and NACA0015 hydrofoil, respectively. *S* denotes the separation point on the GV section. The flow direction is from the left.

4. Summary

At higher angles of incidence the GV produces a more intensive turbulent wake than the NACA foil due to the flow separation from the GV surface and consequent appearance of a second maximum in the fluctuating velocity profiles at quasi-stable regimes. Besides, our experimental results exhibit the axisymmetric cloud shedding process and prove the existence of the cross instability which existence seems to be independent on the test body shape and its aspect ratio.

Acknowledgments

The research was funded by a grant from the Russian Scientific Fund (Project No. 14-29-00203) through Novosibirsk State University.

References

[1] Franc J P and Michel J M 1985 Attached cavitation and the boundary layer: experimental investigation and numerical treatment *J. Fluid Mech.* **154** 63–90

[2] Foeth E-J, van Terwisga T and van Doorne C 2008 On the collapse structure of an attached cavity on a three-dimensional hydrofoil *ASME J. Fluids Eng.* **130(7)** (071303)–9

[3] Ji B, Luo X W, Arndt R E A, Peng X and Wu Y 2015 Large eddy simulation and theoretical investigations of the transient cavitating vortical flow structure around a NACA66 hydrofoil *Int. J. Multiphase Flow* **68** 121–34

[4] Kubota A, Kato H, Yamaguchi H and Maeda M 1989 Unsteady structure measurement of cloud cavitation on a foil section using conditional sampling technique *ASME J. Fluids Eng.* **111(2)** 204–10

[5] Astolfi J-A, Dorange P, Billard J-Y and Cid Tomas I 2000 An experimental investigation of cavitation inception and development on a two-dimensional Eppler hydrofoil *ASME J. Fluids Eng.* **122(1)** 164–73

[6] Huang B, Young Y L, Wang G and Shyy W 2013 Combined experimental and computational investigation of unsteady structure of sheet/cloud cavitation *ASME J. Fluids Eng.* **135(7)** (071301)–16

[7] Kravtsova A Yu, Markovich D M, Pervunin K S, Timoshevskiy M V and Hanjalić K 2014 High-speed visualization and PIV measurements of cavitating flows around a semi-circular leading-edge flat plate and NACA0015 hydrofoil *Int. J. Multiphase Flow* **60** 119–34

[8] Decaix J and Goncalvès E 2013 Investigation of three-dimensional effects on a cavitating Venturi flow *Int. J. Heat Fluid Flow* **44** 576–595